Dalton Transactions

Accepted Manuscript

ROYAL SOCIETY OF CHEMISTRY

www.rsc.org/dalton

Journal Name

RSCPublishing

ARTICLE

Synthesis, Spectroscopic and Electrochemical Studies of Phosphoryl and Carbomethoxyphenyl Substituted Corroles and their Anion Detection Properties

Cite this: DOI: 10.1039/x0xx00000x

Received
Accepted

DOI: 10.1039/x0xx00000x

www.rsc.org/

Pinky Yadav and Muniappan Sankar*

The synthesis, electrochemical studies and anion detection properties of triphosphoryl (**2**) and triester corroles (**3**) are reported and compared with triphenylcorrole (**1**). These corroles exhibited typical acid-base binding behaviour in CH_3CN and converted to monoprotonated and dianionic species respectively. **2** have shown ~30 fold lower K_{eq} values for monoprotonation than that of **1** in TFA/CH_3CN medium. Detection ability of these corroles was also tested in acetonitrile towards various anions. The observed spectral changes in free base corroles (**1-3**) are due to anion induced deprotonation rather than the hydrogen bonding interaction between the imino protons of corrole moiety with anions. **2** and **3** have shown higher equilibrium constants with F^- ion (4.7×10^3 fold higher for **2** and 9.7×10^3 fold higher for **3**) as compared to **1** and being able to detect 0.06 μM of F^- ion. Cu(III) and Ag(III) complexes of **2** and **3** exhibited anodic shift by ~250 mV in first ring oxidation and ~100-150 mV in metal centred reduction as compared to Cu(III) and Ag(III) complexes of **1**. The anodic shift in the redox potentials, lower protonation constants and higher detection limit of anions have been explained in terms of electron withdrawing nature of the diethylphosphite and carbomethoxy substitutents at the *meso*-phenyl positions of the corrole ring.

1. Introduction

Johnson and Kay discovered the corrole macrocycle as a byproduct during the synthesis of vitamin B_{12} in the late 1960s.[1] Corroles started their big career after successful synthesis of triaryl corroles by Paolesse et al and Gross et al at the same time.[2,3] After that the synthetic methodology about corroles has improved significantly.[4] The development of corroles has led to the new version of fully aromatic corrin ring.[5-10] The direct pyrrole-pyrrole linkage which is responsible for their unique physico-chemical properties. Unlike porphyrins, corroles can stabilize the higher oxidation state of metal centers.[10-11] Further, the low valent metal complexes are extremely reactive when chelated by corroles and the opposite holds true for the high valent counter parts. Applications of these metal complexes have been profusely described in the areas of catalysis,[12-18] sensors,[19-20] light- harvesting,[21] DSSC,[22-23] medicine[24] and nonlinear optics (NLO).[25-27]

Department of Chemistry, Indian Institute of Technology Roorkee, Roorkee – 247667, India.

Electronic supplementary information (ESI) available: Figures of optical absorption and emission spectra, ^{1}H NMR spectra, MALDI-TOF mass spectra, UV-Visible spectral titrations for protonation, deprotonation and anion binding studies and cyclic voltammograms of free base corroles.

Sulphonic, phosphonic and carboxylic acid substituted porphyrins show good efficiency in dye sensitized solar cells. Recently β-substituted carboxy[23] or sulphonic acid[22] substituted corroles were used in dye sensitized solar cells. Phosphorylporphyrins have been reported as structural building blocks for supramolecular assemblies.[28-31] Porphyrins substituted with diethoxyphosphoryl groups at *meso*-position of ring or *para*-position of *meso*-phenyl ring show aggregation tendency in solutions. Corroles exhibit interesting physical and chemical properties than porphyrins because of their lower symmetry (C_{2V}).

Corroles can be deprotonated easily due to their high NH-acidity as compared to porphyrins which require vigorous conditions. Corrole forms a stable dianion after abstraction of two protons by strong base such as TBAOH which shows typical characteristics of aromatic compounds.[32] UV-Visible spectrum obtained after monoprotonation of macrocycle shows aromatic nature whereas in concentrated acids it loses the aromatic nature since the second proton is attached to the *meso*-position of macrocycle.[32-37,42]

In recent years, several studies have been carried out in order to explore different fluorescent materials for the development of chemical sensors. In general, corroles show intense absorption and emission in the visible region, good photostability in various solvents and high NH-acidity. All these characteristics of corroles are useful and quite interesting in anion sensor[19] and pH sensor[39] applications. Anion sensing plays an important role in environmental science and biochemistry. As an example, F^- ion is an important

anion in human body which prevents dental caries and maintains solidity of bones. Anion sensing based on porphyrin and corrole receptors are of current interest.[19,40-42] Recently, Cavaleiro and co-workers have studied the anion sensing properties using free base 5,10,15-tris(pentafluorophenyl)corrole (H_3TF_5PCor) and its derivatives.[20] In this paper we report the synthesis, electronic spectral, electrochemical redox properties and anion detection abilities of corroles bearing diethoxyphosphoryl and carbomethoxy groups at *para*-position of *meso*-phenyl ring. To the best of our knowledge, this is the first report on corroles describing the correct mechanism of anion detection (anion induced deprotonation rather than H-bonding) and showing lower detection limit towards basic anions such as fluoride, acetate and dihydrogenphosphate ions.

Experimental section

Chemicals

4-Bromobenzaldehyde, 4-carbomethoxybenzaldehyde and $Pd(PPh_3)_4$ were purchased from Alfa Aesar and used as received. Et_3N, hexane and CH_3CN were dried and distilled over CaH_2. $CHCl_3$ and toluene were dried and distilled over P_2O_5. 5,10,15-triphenylcorrole (**1**) and 5,10,15-tris(4'-carbomethyphenyl)corrole (**3**) were synthesized according to reported literature.[4] Tetrabutylammonium salts (TBAX, X = F, Cl, Br, I, CH_3COO, H_2PO_4, HSO_4, PF_6 and ClO_4) were used as received from Alfa Aesar. We have calculated the limit of detection (LOD) and the limit of quantification (LOQ) for anions by **2** and **3** using formula LOD = 3.3 SD/S and LOQ = 10 SD/S where SD stands for standard deviation of blank, S stands for slope.[43]

Instrumentation

UV-Visible and fluorescence spectra were recorded using Cary 100 spectrophotometer and Hitachi F-4600 spectroflurometer respectively. All ^{1}H NMR measurements were performed using Bruker AVANCE 500 MHz spectrometer in $CDCl_3$. MALDI-TOF mass spectra were measured using a Bruker UltrafleXtreme-TN MALDI-TOF/TOF spectrometer using dithranol as a matrix. The ESI Mass spectrum of **2** was recorded using Bruker daltanics-microTOF instrument in negative ion mode and the elemental analysis were carried out on Elementar vario EL III instrument. Electrochemical measurements were carried out with a BAS Epsilon electrochemical workstation. A three electrode system was used consisted of a GC Working electrode, Ag/AgCl reference electrode and a Pt-wire counter electrode. The concentrations of all corroles employed were ~1 mM. All measurements were performed in triple distilled CH_2Cl_2 which was purged with Ar gas, using 0.1 M TBAP as the supporting electrolyte. Protonation, deprotonation and anion induced deprotonation of corrole **1-3** were carried out in CH_3CN at room temperature. The equilibrium constants, K_{eq} were evaluated using the reported procedure.[44] The equation for the evaluation of the K_{eq} is given below

$$1/K_{eq} = [base]\{[corrole]L(\varepsilon_c-\varepsilon_{ca})/(A_n-A_0)-1\}$$

Where ε_c and ε_{ca} are the molar extinction coefficients of the free base corrole and corrole-anion complex, respectively. A_0 and A_n are the absorbance values in absence and in presence of added anion at a particular wavelength. L is the path length of the cell employed. A plot of $[anion]^2$ versus $[anion]^2/A_n-A_0$ was yielded a straight line. Using the above equation, the K_{eq} can be evaluated by taking the negative of the 1/intercept. The stoichiometry of the binding was analysed by Hill method.[45] A Hill plot was constructed by the plot of $\ln[(A_0-A_n)/(A_n-A_f)]$ against ln[anion] where A_0 and A_n are the absorbance values of corrole employed and corrole-anion complex, respectively at a given concentration of the anion added. A_f denotes the absorbance of the completely bound corrole-anion complex at a particular wavelength. The slope of the line is expected to yield two for one-to-two stoichiometry between the corrole and the added anion. The above-mentioned method was employed for protonation and deprotonation studies.

Synthesis of (4-diethoxyphosphoryl)benzaldehyde[46]

1g of 4-bromobenzaldehyde (5.40 mmol) was taken in a 100 mL two neck RB flask. To this, dry toluene (8 mL), dry triethylamine (8 mL) and diethyl phosphite (0.773 mL, 6 mmol) were added and purged with Ar gas for 2 minutes. Finally, $Pd(PPh_3)_4$ (0.31 gm, 0.27 mmol) was added and heated to 90 °C for 24 hrs under Argon atmosphere. The reaction mixture was cooled to room temperature and the solvent mixture was evaporated to dryness under vacuum, redissolved in $CHCl_3$ (70 mL), washed with distilled water (3×100 mL) followed by brine solution (100 mL) and finally dried over sodium sulphate. The crude product was purified on silica column using $CHCl_3$/EtOAc (7:3, v/v) as eluent. The yield of (4-diethoxy phosphoryl)benzaldehyde was found to be 0.8 g (61%).

^{1}H NMR ($CDCl_3$): δ (ppm) 10.05 (s, 1H, CHO), 7.62 (m, 2H, *o*- ph-H), 7.42 (td, J = 8 Hz, J = 2.5 Hz, 2H, *m*-ph-H), 4.12 (m, 4H, -OCH_2), 1.30 (t, J = 7.1 Hz, 6H, -CH_3).

5,10,15-tris(4'-diethoxyphosphorylphenyl)corrole(H_3TPPC) [2]

(4-diethoxyphosphoryl)benzaldehyde (1 gm, 4.13 mmol) and pyrrole (0.570 mL, 8.26 mmol) were dissolved in 400 mL of water and MeOH (1:1, v/v) mixture. Subsequently, 3.5 mL of conc. HCl (36%) was added drop wise and stirred for 3 hrs at room temperature. Then the reaction mixture was extracted with 100 mL of $CHCl_3$, washed twice with water (2 × 100 mL), dried over Na_2SO_4, and diluted with $CHCl_3$ to 270 mL. To this, *p*-chloranil (1 gm, 1 mmol) was added and then refluxed for 1 hr. The crude product was purified on silica column using 3% MeOH in $CHCl_3$ as eluent. Yield of **2** was found to be 10% (0.130 gm, 0.139 mmol).

UV/Vis (CH_2Cl_2): λ_{max} (nm) ($\varepsilon\times10^{-3}$ L mol^{-1} cm^{-1}) 419 (66.0), 575 (11.2), 617 (8.1), 647 (6.6). ^{1}H NMR in $CDCl_3$ (500 MHz): δ(ppm) 9.04 (d, 2H, J = 4.15 Hz, β-pyrrole-H), 8.89 (d, 2H J = 4.7 Hz, β-pyrrole-H), 8.63 (d, 2H, J = 4.1 Hz, , β- pyrrole-H), 8.56 (d, 2H, J = 4.7 Hz, , β- pyrrole-H), 8.46-8.50 (m, 4H, *meso-o*-phenyl-H), 8.18-8.32 (m, 8H, *meso-o and m*-phenyl-H), 4.30-4.42 (m, 12H, -OCH_2), 1.51 (t, 18H, J = 6.47 Hz, -CH_3) ESI-MS (m/z): found 971.272 [M+Cl$^-$], calcd. 971.268. Anal. calcd. for $C_{49}H_{53}N_4O_9P_3$: C, 62.95; H, 5.71; N, 5.99%. Found: C, 62.70; H, 5.95; N, 6.15%.

Preparation of Cu(III) and Ag(III) Corroles

Free base corrole (0.050 gm, 0.0535 mmol) was dissolved in 30 mL $CHCl_3$. To this, 10 equiv. of copper(II) acetate monohydrate or silver(I) acetate in 8mL MeOH was added and stirred at room temperature for 1 hr. Then the reaction mixture was evaporated to dryness, redissolved in minimum amount of $CHCl_3$ (15 mL) and washed with distilled water (50 mL). The organic layer was dried over Na_2SO_4 and purified on silica column using 1% MeOH in $CHCl_3$ as eluent. The yields of **2a**, **2b**, **3a** and **3b** were mentioned below along with their characterisation data.

5,10,15-tris(4'-diethoxyphosphorylphenyl))corrolato Cu(III) [2a]

UV/Vis (CH_2Cl_2): λ_{max} (nm) ($\varepsilon\times10^{-3}$ L mol^{-1} cm^{-1}) 412(54.9), 536(4.2), 617(2.9). ^{1}H NMR in $CDCl_3$ (500 MHz): δ(ppm) 7.90-7.96

(m, 8H, *meso-o, m and p*-phenyl-H), 7.84-7.86 (m, 4H, *meso-o*-phenyl-H), 7.74-7.75 (m, 2H, β-pyrrole-H), 7.61 (d, 2H, J = 3.8 Hz, β-pyrrole-H), 7.32 (d, 2H, J = 3.9 Hz, β-pyrrole-H), 7.20 (d, 2H, J = 4.4 Hz, β-pyrrole-H), 4.28-4.12 (m, 12H, $-OCH_2$), 1.41 (at, 18H, J = 4.7 Hz, $-CH_3$) MALDI-TOF-MS (m/z): 995.420 $[M]^+$ (calcd, 995.425). The yield of **2a** was found to be 56 % (30 mg, 0.03 mmol).

5,10,15-tris(4'-diethoxyphosphorylphenyl)corrolatoAg(III) [2b]

UV/Vis (CH_2Cl_2): λ_{max} (nm) (ε × 10^{-3} L mol^{-1} cm^{-1}) 429(57.5), 561(8.3), 583(15.1). ^1H NMR in $CDCl_3$ (500 MHz): δ(ppm) 9.26 (d, 2H, J = 4.0 Hz, β-pyrrole-H), 8.99 (d, 2H, J = 4.5 Hz, β-pyrrole-H), 8.79 (d, 2H, J = 4.0 Hz, β-pyrrole-H), 8.75 (d, 2H, J = 5.0 Hz, β-pyrrole-H), 8.41-8.44 (m, 4H, *meso-o*-phenyl-H), 8.33-8.35 (m, 2H, *meso-o*-phenyl-H), 8.29-8.25 (m, 6H, *meso-m*-phenyl-H), 4.43-4.36 (m, 12H, $-OCH_2$), 1.52 (t, J = 6.5 Hz, 18H, $-CH_3$) MALDI-TOF-MS (m/z): 1057.740 $[M{\bullet}H_2O]^+$ (calcd, 1057.757). The yield of **2b** was found to be 45 % (25 mg, 0.024 mmol).

5,10,15-tris(4'-carbomethoxyphenyl)corrolato Cu(III) [3a]

UV/Vis (CH_2Cl_2): λ_{max} (nm) (ε × 10^{-3} L mol^{-1} cm^{-1}) 414(47.8), 541(3.4), 626(2.3). ^1H NMR in $CDCl_3$ (500 MHz): δ(ppm) 8.20 (d, 4H, J = 7.5 Hz, *meso-o*-phenyl-H), 8.17 (d, 2H, J = 8.0 Hz, *meso-o*-phenyl-H), 7.96 (d, 2H, J = 3.2 Hz, β-pyrrole-H), 7.84 (d, 4H, J = 8.1 Hz, *meso-m*-phenyl-H), 7.74 (d, 2H, J = 8.1 Hz, *meso-m*-phenyl-H), 7.62 (d, 2H, J = 4.3 Hz, β-pyrrole-H), 7.34 (d, 2H, J = 4.3 Hz, β-pyrrole-H), 7.21 (d, 2H, J = 4.6 Hz, β-pyrrole-H), 4.02 (s, 6H, $-OCH_3$), 4.01 (s, 3H, $-OCH_3$). MALDI-TOF-MS (m/z): 761.348 $[M]^+$ (calcd, 761.273). The yield of **3a** was found to be 66 % (36 mg, 0.047 mmol) .

5,10,15-tris(4'-carboxymethylphenyl)corrolatoAg(III) [3b]

UV/Vis (CH_2Cl_2): λ_{max} (nm) (ε × 10^{-3} L mol^{-1} cm^{-1}) 428(64.5), 527(4.5), 584(17.4). ^1H NMR in $CDCl_3$ (500 MHz): δ(ppm) 9.07 (d, 2H, J = 4.3 Hz, β-pyrrole-H), 8.92 (d, 2H, J = 4.7 Hz, β-pyrrole-H), 8.68 (d, 2H, J = 4.5 Hz, β-pyrrole-H), 8.66 (d, 2H, J = 4.5 Hz, β-pyrrole-H), 8.49 (d, 4H, J = 8.1 Hz, *meso-o*-phenyl-H), 8.45 (d, 2H, J = 8.1 Hz, *meso-o*-phenyl-H), 8.34 (d, 4H, J = 8.1 Hz, *meso-m*-phenyl-H), 8.23 (d, J = 8.1 Hz, 2H, *meso-m*-phenyl-H), 4.12 (s, 6H, $-OCH_3$), 4.11 (s, 3H, $-OCH_3$). MALDI-TOF-MS (m/z): 805.373 $[M]^+$ (calcd, 805.589). The yield of **3b** was found to be 56 % (32 mg, 0.039 mmol).

Chart 1 Molecular structures of synthesized corroles.

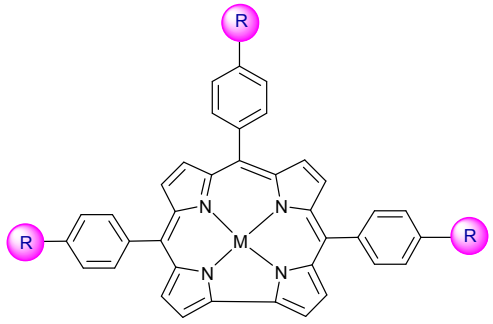

1 M = 3H, R = H	1a M = Ag, R = H	1b M = Cu, R = H
2 M = 3H, R = $PO(OEt)_2$	2a M = Ag, R = $PO(OEt)_2$	2b M = Cu, R = $PO(OEt)_2$
3 M = 3H, R= $COOCH_3$	3a M = Ag, R= $COOCH_3$	3b M = Cu, R= $COOCH_3$

Results and discussion

Synthesis and Characterization

We have synthesized different free base corroles (**1-3**) and their Cu(III) and Ag(III) complexes are shown in chart 1. **1** and **3** were synthesized according to the procedure described by Gryko in H_2O-MeOH mixture.[4a] Initially, we tried to synthesize 5,10,15-tris(4'-diethoxyphosphorylphenyl)corrole *via* Pd-catalysed coupling reaction using 5,10,15-tris(4'-bromophenyl)corrole and diethylphosphite by refluxing in ethanol under argon atmosphere as reported for the synthesis of phosphorylporphyrins in the literature.[29] Unfortunately, the reaction yielded an inseparable mixture of products with very low yield (< 0.5%). Alternatively, we synthesized 4-diethoxyphosphorylbenzaldehyde[46] and then condensed it with pyrrole in water-methanol mixture[4a] and the yield was found to be 10%. (Scheme 1)

Scheme 1 Synthesis of triphosphorylphenylcorrole (**2**) and its metal complexes (**2a** and **2b**).

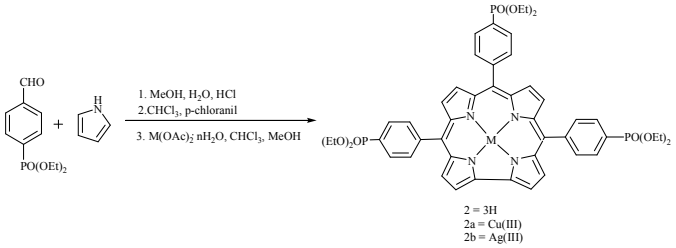

Ag(III) and Cu(III) metal complexes were prepared by reacting free base corroles and corresponding metal acetates in $CHCl_3$/methanol mixture as shown in scheme 1. All the synthesized corroles were characterized by UV-Visible, fluorescence, ^1H NMR and mass spectroscopic techniques.

The UV-Visible spectral features of **2** and **2a-b** in CH_2Cl_2 are shown in Fig. 1a. Table 1 shows the optical absorption spectral data of synthesized corroles. Also the electronic absorption spectra of **3** and **3a-b** are shown in supporting information (Fig. S1). **2** shows a Soret

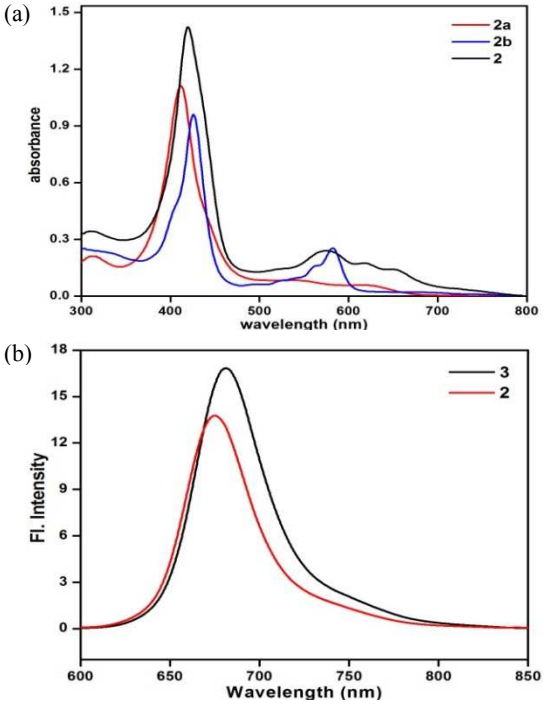

Fig. 1 (a) UV-Visible spectra of **2** and **2a-b** in CH_2Cl_2, (b) Fluorescence spectra of **2** and **3** in CH_2Cl_2.

band at 419 nm and three Q bands at 575, 617 and 647 nm which are marginally red shifted than that of **1** and 5 nm blue-shifted than **3**. Fig. 2b shows the emission spectra of **2** and **3** in CH_2Cl_2 showing the maxima at 678 and 686 nm respectively. **2** exhibited 7 nm red shift and 8 nm blue-shifted as compared to **1** and **3** respectively.

Table 1 Optical absorption spectral data of compound **1-3** and their metal complexes (λ_{max} (nm) ($\varepsilon \times 10^{-3}$ L mol^{-1} cm^{-1})) in CH_2Cl_2.

Corrole	B band (nm)	Q bands (nm)
2	419(66.0)	575(11.2), 617(8.1), 647(6.6)
2a	412(54.9)	536(4.1), 617(2.9)
2b	429(57.5)	561(8.3), 583(15.1)
3	424(52.5)	579(9.3), 622(6.6), 653(4.9)
3a	414(47.8)	542(3.4), 621(2.3)
3b	428(64.5)	526(4.5) ,584(17.4)

^{1}H NMR of **2** shows the characteristic four doublets corresponding to β-protons of corrole macrocycle. A multiplet at 4.30-4.42 ppm (12 H) and a triplet at 1.51 ppm (18 H) confirm the diethoxyphosphoryl group at the *meso*-phenyl position of the corrole. ^{1}H NMR signals of **2b** showed downfield shift (0.2 - 0.3 ppm) than **2** and **2a**, possibly due to enhanced planarity in Ag corrole complexes.[47] The ^{1}H NMR spectra of **2**, **2a**, **2b** and **3b** are shown in supporting information (figures S2-S5). Aggregation behaviour of **2** and **3** were studied using UV-Visible spectrophotometer at various concentrations (0.53 -1.59 × 10^{-5} M) in CH_2Cl_2. These corroles did not show any considerable changes which means that **2** and **3** do not aggregate in CH_2Cl_2 at 10^{-5} M concentration whereas the broad peaks in ^{1}H NMR spectra of **2** and **3** at ~ 0.015 M in $CDCl_3$ indicates the aggregation behaviour of these corroles at high concentration. The MALDI-TOF mass spectra of **2a**, **2b, 3a** and **3b** are shown in supporting information (figures S6-S9) and the experimental mass values are in accordance with the calculated mass values for [M^+].

Protonation studies

Protonation studies of free base corroles (**1-3)** were studied in CH_3CN using trifluroacetic acid (TFA) as titrating agent. Figure 2 shows the UV-Visible spectral changes of **3** with increasing the concentration of TFA. The absorbance at 421 nm of **3** had concomitant decrement and a new shoulder rises at 429 nm with 8 nm red-shift. Similarly, **3** showed a concomitant decrement in the absorbance at 582 nm and rising a new band at 680 nm accompanied with a red-shift of 22 nm in Q band as shown in Fig. 2. In all cases, we obtained monoprotonated corrole species which was further confirmed by Hill plot showing the slope value of 1 (Fig. S10a in ESI). All the monocationic corroles (scheme 1) exhibited stable aromatic nature as confirmed from their UV-Visible spectral features. A representative plot for the evaluation of K_{eq} for the protonation of **2** is shown as an inset in figure 2. Also a similar behaviour was observed for **1** and **3** as shown in Fig. S11 in ESI. Table 2 lists the protonation constants for **1-3** in CH_3CN. The highest logK was observed for **1** (4.93) and lowest for **2** (3.75), which suggests that the electron withdrawing nature of phosphoryl groups makes it difficult to protonate the inner core nitrogen of corrole **2**. The similar results were obtained for **3** as compared to **1**. The protonation constants (logK) follow the trend as expected: **1** > **3** > **2.**

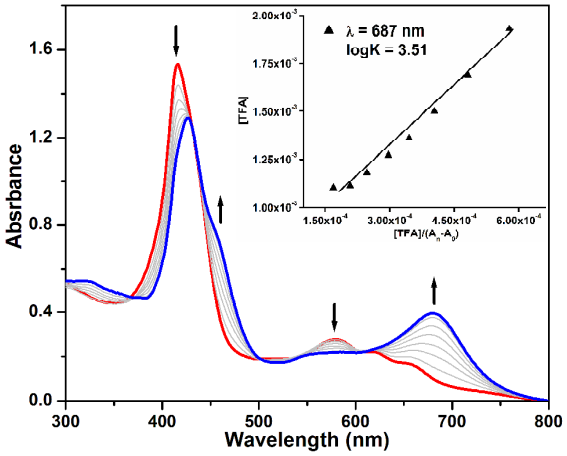

Fig. 2 UV-Visible spectral titration of **2** (2.13×10^{-5} M) with μM concentration of TFA in acetonitrile. Inset shows a plot between [TFA] and [TFA]/(A_n-A_0).

Table 2 Protonation and deprotonation constant of **1-3** in CH_3CN.

Corrole	TFA			TBAOH		
	K	logK	n	β_2	logβ_2	n
1	8.52×10^4	4.93	1	5.76×10^9	9.76	2
2	0.32×10^4	3.51	1	1.89×10^9	9.27	2
3	0.94×10^4	3.97	1	1.91×10^9	9.28	2

Deprotonation Studies

UV-Visible titration method was employed to determine the deprotonation constants of **1-3** in CH_3CN using tetrabutylammonium hydroxide (TBAOH) as a base and the spectral changes of **2** during the course of titration are shown in Figure 3. The absorbance decreased at 421 nm with the emergence of a new B band at 442 nm accompanied by 21 nm red shift. A similar behaviour was observed for Q-bands (decrement in the absorbance at 583 nm and a concomitant increase in absorbance at 646 nm) as shown in figure 3. Inset shows a straight line between $[TBAOH]^2/A_0$-A_n versus $[TBAOH]^2$ from which β_2 value was calculated for the deprotonation of **2**. Hill plot refers to 1:2 stoichiometry or two proton abstraction by the base (TBAOH) as shown in figure S10b (ESI) and scheme 2. Deprotonation spectral changes of **3** are shown in Figure S12 in ESI. The deprotonation constants of **1-3** are summarized in table 2. The logβ_2 value of **2** (9.27) is marginally less than free base β-octaethylcorrole (9.50) and close to tris(*p*-methylphenyl)corrole (9.2).[36] This suggests that the acidity of imino protons of **2** and **3** are comparable to that of **1** which is different from the expected trend.

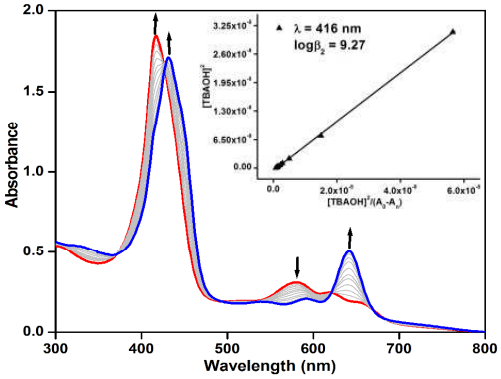

Fig. 3 UV-Visible spectral changes in **2** (2.59×10^{-5} M) during addition of TBAOH in acetonitrile (inset shows a plot between $[TBAOH]^2$ and $[TBAOH]^2/(A_0-A_n)$).

Anion detection

Anion detection by **1-3** were studied in CH_3CN with various spherical halide ions such as F^-, Cl^-, Br^- and I^- and bulky anions such as CH_3COO^-, $H_2PO_4^-$, HSO_4^-, PF_6^- and ClO_4^- using UV-Visible spectrophotometer with the addition of aliquot anion TBA salts. The free base corroles (**1-3**) were selectively bind with F^-, CH_3COO^- and $H_2PO_4^-$ ions and show considerable red-shift (10-15 nm) in the UV-Visible spectra as shown in Figures 4 and S13 (ESI) whereas no shifts were observed for other anions. There are two possibilities of

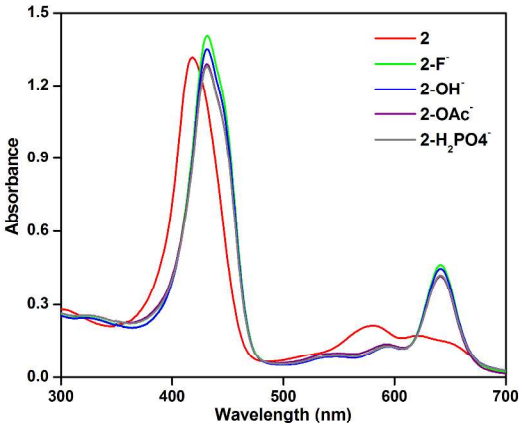

Fig. 4 Absorption spectral changes of 2 with μM quantities of base and anions.

corrole and anion interaction; (i) anions may have strong hydrogen bonding with NH moieties of corrole core or (ii) these basic anions can abstract the acidic proton of NH group that is called anion induced deprotonation. The UV-Visible spectral changes of receptor **2** with different anions were same as that of TBAOH (fig. 4). These results indicate that spectral changes were most probably due to the deprotonation of NH moiety by basic anions (F^-, CH_3COO^- and $H_2PO_4^-$) and not through hydrogen bonding. The spectrophotometric titration of **2** with fluoride ion is shown in Fig. 5. As we increase the concentration of F^- ion, a decrement in the absorbance is observed at 417 nm and 581 nm and a concomitant increment in absorbance at 432 nm and 642 nm respectively with the isosbestic points at 425 nm and 618 nm. The Equilibrium constant for F^- ion binding was calculated using a plot of $[anion]^2$ versus $[anion]^2/A_n\text{-}A_0$ as shown in Figure 5 inset. Hill plot (fig. S13b in ESI) shows a straight line between $\log[F^-]$ and $\log(A_0\text{-}A_n/A_f\text{-}A_n)$ having slope value of 2 which indicates 1:2 (corrole-to-anion) stoichiometry as shown in scheme 2. A similar behavior was observed for **3** as shown in Figure S14 in ESI. The similar spectral changes were obtained for CH_3COO^- and $H_2PO_4^-$ with **1-3** (ESI Fig. S15-S16). The equilibrium constants of **1-3** with different anions are summarized in Table 2. The F^-, CH_3COO^- and $H_2PO_4^-$ induced deprotonation is fully reversible as evidenced from the addition of CH_3OH. The addition of polar protic solvent such as CH_3OH results the gradual decrease in absorbance as reflected in UV-Visible spectral studies (see Fig. S17 in ESI). This is possibly due to the competition between the protic solvent versus anions (F^-, CH_3COO^- and $H_2PO_4^-$) with NH moiety. Moreover, the

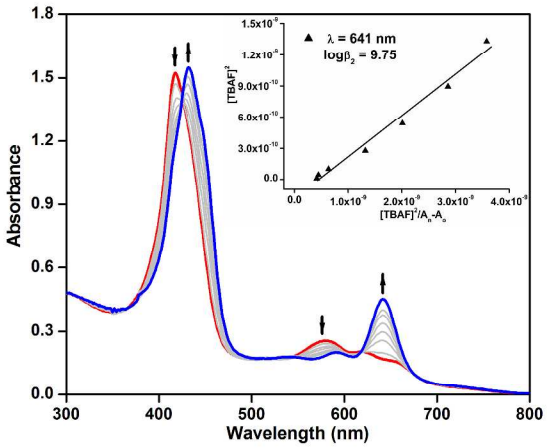

Fig. 5 UV-Visible spectral titration **2** (2.13×10^{-5} M) with TBAF (inset shows a plot between $[TBAF]^2$ and $[TBAF]^2/(A_n\text{-}A_0)$.

presence of high amount of protic solvent disfavors the formation of deprotonated receptor **2.**

2 and **3** have shown higher equilibrium constants with F^- ion (4.7×10^3 fold higher for **2** and 9.7×10^3 fold higher for **3**) as compared to that of **1**. The electron withdrawing nature of diethoxyphosphoryl and carbomethoxy groups make the corroles **2** and **3** more acidic which is responsible for deprotonation of inner core NH protons by basic anions as compared to **1**. No Changes were observed for **1-3** in the presence of Cl^-, Br^-, I^-, HSO_4^-, PF_6^- and ClO_4^-. This means that the receptor provides selectivity F^-, CH_3COO^- and $H_2PO_4^-$ which is solely based upon its deprotonation and is related to the factors (a) intrinsic acidity of receptor, (b) basicity of anion and (c) polarity of the solvent.[48] Imino protons of free base corroles (**2** and **3**) are highly acidic in nature and hence they are sensitive for basic anions such as F^-, CH_3COO^- and $H_2PO_4^-$ ions. The small ionic size (1.3 Å) and the high electronegativity (4.1) of fluoride ion are responsible for easy deprotonation of NH group as compared to other anions. Moreover, the size of the corrole core (2.50 Å) is compatible with the fluoride

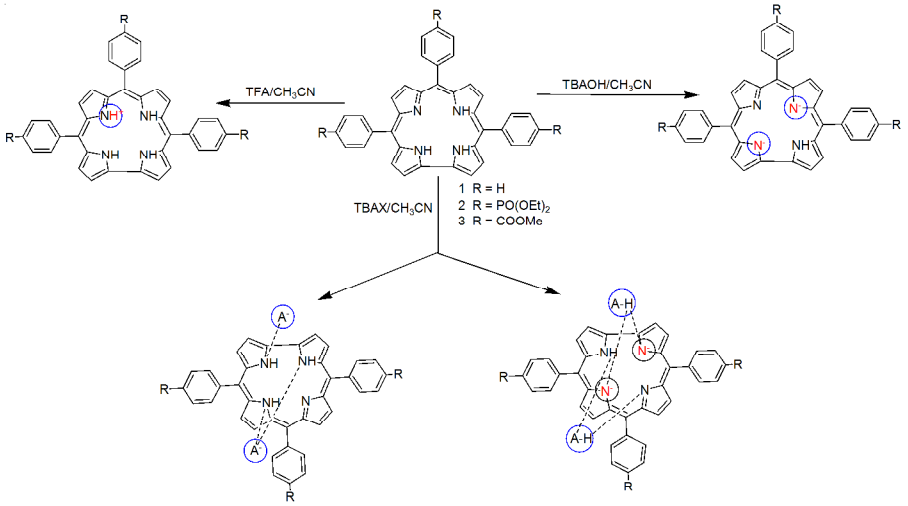

Scheme 2 Schematic representation of protonation, deprotonation and anion binding with **1- 3**.

ion size which is responsible for the higher equilibrium constants.

The detection limit (LOD) and quantification limit (LOQ) for F^-, CH_3COO^- and $H_2PO_4^-$ were calculated in presence of **1-3** in CH_3CN. **2** shows more sensitivity towards F- ion, LOD for **2** was found to be 0.06 μM and LOQ 0.17 μM. **3** shows higher sensitivity towards basic anions CH_3COO^- and $H_2PO_4^-$ with very high detection limit of 0.04 μM. These results suggest that **2** and **3** are very much sensitive for anion detection as compared to the reported corroles.[20a]

Table 3 Equilibrium constants[a] of **1-3** while addition of μM quantities of anions in CH_3CN.

compound	anion	logβ_2	A : L	LOD (μM)	LOQ (μM)
1	F^-	6.06	1:1	0.50	2.43
	CH_3COO^-	10.53	2:1	0.18	6.48
	$H_2PO_4^-$	9.39	2:1	0.17	6.90
2	F^-	9.74	2:1	0.06	0.17
	CH_3COO^-	10.80	2:1	0.05	0.14
	$H_2PO_4^-$	10.27	2:1	0.05	0.14
3	F^-	10.05	2:1	0.06	0.19
	CH_3COO^-	9.63	2:1	0.04	0.12
	$H_2PO_4^-$	9.50	2:1	004	0.11

[a]within the error ± 0.14.

Electrochemistry

To probe the influence of the *meso*-phenyl substituents on the π-electronic properties of the corrole ring system, the electrochemical redox behaviours of these corroles were studied by cyclic voltammetric analysis. **1-3** were showing two reversible oxidations and one irreversible reduction as shown in fig. S18 in ESI. **2** and **3** exhibited anodic shift in their first oxidation (~120 mV) and reduction (160-400 mV) potentials as compared to **1.** Since the anion radicals of **1-3** formed after electrochemical reduction are unstable and undergo disproportionation hence we used metal complexes to probe further. The CVs of Ag(III) and Cu(III) complexes of **1-3** are shown in Fig. 5. **1b** shows three oxidations and two reductions as reported in literature[47] whereas **2b** and **3b** show two ring centred oxidations and one metal centred reduction (Table 3). The first oxidation potentials of **2a-b** and **3a-b** are more anodically shifted (~250 mV) as compared to **1a-b**. The metal centred reductions of **2a** and **3a** are anodically shifted (~100-150 mV) as compared to **1a.** The anodic shift of redox potentials is ascribed to strong electron withdrawing nature of diethoxyphosphoryl and carbomethoxy groups.

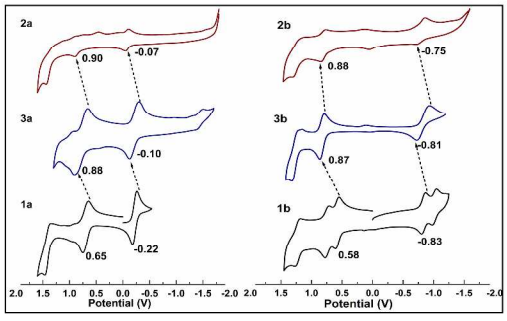

Fig. 6 Cyclic Voltammograms of **1b-3b** in CH_2Cl_2 containing 0.1M TBAP with a scan rate of 100 mV/s.

The higher reduction potentials of Ag(III) corroles as compared to Cu(III) corroles is due to more electropositive nature of silver metal. For the Hammet equation $E_{1/2} = 3\sigma\rho$, the plot of first ring oxidation and metal centred reduction *versus* the Hammet parameter (σ_p) of the substituents was examined to delineate the role of substituents on corrole π-system and they exhibited linear trend as shown in fig. 6. The reaction constant, ρ for the first oxidation *versus* σ_p was found to be higher (195 mV) for Ag corroles relative to that of Cu corroles (165 mV) which indicates the higher reactivity of Ag corrole towards oxidation. The reaction constant obtained from the plot of reduction potential versus σ_p was found to be higher of Cu corroles (91 mV) as compared to Ag corroles (44 mV) which indicates higher tendency towards reduction for Cu corroles. These results clearly indicate that diethoxyphosphoryl and carbomethoxy corroles are electron deficient in nature so that they show highest equilibrium constant towards the basic anions.

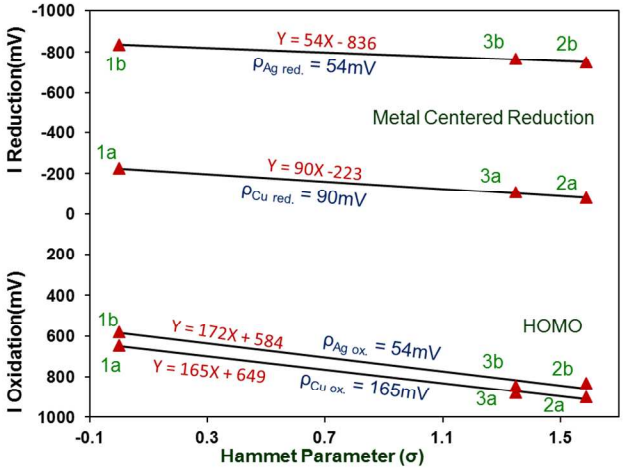

Fig. 7 The Plot of Hammet parameter (3σ) *versus* the first ring oxidation and the metal centered reduction of Cu(III) and Ag(III) complexes of **1-3**.

Table 3 Electrochemical redox data for compound **1-3** and their metal complexes in CH_2Cl_2.

corrole	3σ	Oxidation			Reduction	
		I	II	III	I	II
1a	0	648	1420	-	-223	-
2a	1.59	904	1385	-	-76	-
3a	1.35	882	-	-	-105	-
1b	0	580	744	1239	-836	-1017
2b	1.59	884	1372	-	-752	-
3b	1.35	856	1295	-	-800	-

Conclusion

We have synthesized a new family of electron deficient corroles and characterized by spectroscopic techniques and electrochemical studies. **2** and **3** exhibited red shifted absorption spectra and a downfield shift in ^1H NMR as compared to **1**. Protonation constant of **2** is ~30 fold lower as compared to **1** reflecting electron withdrawing nature of diethoxyphosphoryl groups. **2** and **3** have shown higher equilibrium constants with F^- ion (4.7×10^3 fold higher for **2** and 9.7×10^3 fold higher for **3**) as compared to **1** and being able to detect 0.06 μM of F^- ion. **2** was also found to be more

sensitive towards CH_3COO^- and $H_2PO_4^-$ ions and allowing to detect 0.05 μM of these anions with the LOQ of 0.14 μM. Tricarbomethoxyphenyl and triphosphorylphenyl substituted metallocorroles exhibited anodic shift of ~250 mV in oxidation and ~100-150 mV in metal centered reduction as compared to **1** due to the electron withdrawing nature of the substituents. The linear trend in Hammet plot also substantiates the effect of substituents on corrole π-system. These results indicate that electron deficient corroles can be utilized as efficient basic anion detectors.

Acknowledgment

We are grateful for the financial support provided by Council of Scientific and Industrial Research (01(2694)/12/EMR-II), Science and Engineering Research Board (SB/FT/CS-015/2012) and Board of Research in Nuclear Sciences (2012/37C/61BRNS/253). PY thanks CSIR for the Junior Research Fellowship (JRF).

REFERENCES

1. A. W. Johnson and I. T. Kay, *J. Chem. Soc*., 1965, 1620.
2. (a) R. Paolesse, L. Jaquinod, D. J. Nurco, S. Mini, F. Sagone, T. Boschi and K. M. Smith, *Chem. Commun*., 1999, 1307-1308 (b) R. Paolesse, S. Nardis, F. Sagone and R. G. Khoury, *J. Org. Chem*., 2001, **66**, 550-556.
3. (a) Z. Gross, N. Galili, L. Simkhovich, I. Saltsman, M. Botoshansky, D. Blaser, R. Boese and I. Goldberg, *Org. Lett.,* 1999, **1**, 599-602 (b) Z. Gross, N. Galili and I. Saltsman, *Angew. Chem. Int. Ed.,* 1999, **38**, 1427-1429.
4. (a) B. Koszarna and D. T. Gryko, *J. Org. Chem.,* 2006, **71,** 3707-3717 (b) C. Capar, L. K. Hansen, J. Conradie and A. Ghosh, *J. Porphyrins Phthalocyanines,* 2010, **14,** 509-512 (c) K. E. Thomas, I. H. Wasbotten and A. Ghosh, *Inorg. Chem*., 2008, **47,** 10469-10478 (d) A. Ghosh, *Angew. Chem. Int. Ed*., 2004, **43**, 1918-1931 (e) E. Steene, A. Dey and A. Ghosh, *J. Am. Chem. Soc*., 2003, **125,** 16300-16309.
5. C. Erlen, S. Will and K. M. Kadish, In *The Porphyrin Handbook*; K. M. Kadish, K. M. Smith and R. Guilard, Eds.; Academic Press: New York, 2000, **2,** 233-300.
6. J. Bendix, I. J. Dmochowski, H. B. Gray, A. Mahammed, L. Simkhovich and Z. Gross, *Angew. Chem. Int. Ed.,* 2000, **39,** 4048-4051.
7. A. Mahammed and Z. Gross, *J. Inorg. Biochem.,* 2002, **88,** 305-309.
8. K. Sorasaenee, P. Taqavi, L. M. Heling, H. B. Gray, E. Tkachenko, A. Mahammed and Z. Gross, *J. Porphyrins Phthalocyanines,* 2007, **11,** 189-197.
9. S. Nardis, D. Monti and R. Paolesse, *Mini Rev. Org. Chem.,* 2005, **2,** 355-372.
10. Z. Gross, *J. Biol. Inorg. Chem.,* 2001, **6,** 733-738.
11. Z. Gross and H. B. Gray, *Comments Inorg. Chem.,* 2006, **27,** 61-72.
12. S. H. Kim, H. Park, M. S. Seo, M. Kubo, T. Ogura, J. Klajn, D. T. Gryko, J. S. Valentine and W. Nam, *J. Am. Chem. Soc.,* 2010, **132,** 14030-14032.
13. H. Y. Liu, M. H. R. Mahmood, S. X. Qiu and C. K. Chang, *Coord. Chem. Rev.,* 2013, **257***,* 1306-1333.
14. Y. Han, Y. M. Lee, M. Mariappan, S. Fukuzumi and W. Nam, *Chem. Commun.,* 2010, **46,** 8160-8162.
15. Z. Gross, L. Simkhovich and N. Galili, *Chem. Commun.,* 1999, 599-600. (b) K.M. Kadish, L. Fremond, F. Burdet, J-M. Barbe, C. P. Gros, and R. Guilard, *J. Inorg. Biochem*., 2006, **100,** 858-868.
16. (a) G. Golubkov, J. Bendix, H. B. Gray, A. Mahammed, I. Goldberg, A. J. DiBilio and Z. Gross, *Angew. Chem., Int. Ed*., 2001, **40,** 2132-2134; (b) H.Y. Liu, T.S. Lai, L. L. Yeung and C. K Chang, *Org. Lett*., 2003, **5,** 617-620.
17. I. Luobeznova, M. Raizman, I. Goldberg and Z. Gross, *Inorg. Chem*., 2006, **45,** 386-394.
18. G. Golubkov and Z. Gross, *J. Am. Chem. Soc*., 2005, **127,** 3258-3259.
19. R. Paolesse, C. D. Natale, A. Macognano, F. Sagone, M.A. Scarselli, P. Chiaradia, V.I. Troitsky, T.S. Berzina and A. D'Amico, *Langmuir,* 1999, **15,** 1268-1274.
20. (a) C. I. M. Santos, E. Oliveira, J. F. B. Barata, M. A. F. Faustino, J. A. S. Cavaleiro, M.G.P.M.S. Neves and C. Lodeiro, *J. Mater. Chem*., 2012, **22,** 13811-13819 (b) C. I. M. Santos, E. Oliveira, J. F. B. Barata, M. A. F. Faustino, J. A. S. Cavaleiro, M. G. P. M. S. Neves, and C. Lodeiro, *Inorg. Chim. Acta*, 2014, **417**, 148-154.
21. R. Paolesse, F. Sagone, A. Macagnano, T. Boschi, L. Prodi, M. Montalti, N. Zaccheroni, F. Bolletta and K.M. Smith, *J. Porphyrins Phthalocyanines,* 1999, **3,** 364-370.
22. D. Walker, S. Chappel, A. Mahammed, J. J. Weaver, B. S. Brunschwig, J. R. Winkler, H. B. Gray, A. Zaban and Z. Gross, J. *Porphyrins Phthalocyanines,* 2006, **10,** 1259-1262.
23. K. Sudhakar, V. Velkannan and L. Giribabu, *Tetrahedron Lett*., 2012, **53,** 991–993.
24. A. Haber, A. Mahammed, B. Fuhrman, N. Volkova, R. Coleman, T. Hayek, M. Aviram and Z. Gross, *Angew. Chem., Int. Ed.,* 2008, **47,** 7896-7900.
25. (a) A. Rebane, M. Drobizhev, N. S. Makarov, B. Koszarna, M. Tasior and D. T. Gryko, *Chem. Phys. Lett.* 2008, **462,** 246-250. (b) P. T. Anusha, D. Swain, S. Hamad, L. Giribabu , T. S. Prashant, S. P. Tewari and S. V. Rao, *J. Phys. Chem. C*, 2012, **116,** 17828-17837.
26. S. Cho, J. M. Lim, S. Hiroto, P. Kim, H. Shinokubo, A. Osuka and D. Kim, *J. Am. Chem. Soc.,* 2009, **131,** 6412-6420.
27. X. Ying, X. Y. Long, M. H. R. Mahmood, Q.Y. Hu, H. Y. Liu and C. K. Chang, *J. Porphyrins Phthalocyanines,* 2012, **16,** 1276–1284.
28. K. E. Borbas, H. L. Kee, D. Holten and J. S. Lindsey, *Org. Biomol. Chem*., 2008, **6,** 187-194.
29. K. M. Kadish, P. Chen, Y. Yu. Enakieva, S. E. Nefedov, Y. G. Gorbunovab, A. Y. Tsivadze, A. Bessmertnykh-Lemeune, C. Stern and R. Guilard, *J. Electroanal. Chem.,* 2011, **656**, 61-71.
30. A. A. Sinelshchikova, S. E. Nefedov, Y. Y. Enakieva, Y. G. Gorbunova, A. Y. Tsivadze, K. M. Kadish, P. Chen, A. Bessmertnykh-Lemeune, C. Stern and R. Guilard, *Inorg. Chem*. 2013, **52,** 999-1008.
31. D. L. Officer, F. Lodato and K. W. Jolley, *Inorg. Chem***.** 2007, **46,** 4781-4783.
32. Y. Fang, K. M. Kadish, P. Chen, Y. Gorbunova, Y. Enakieva, A. Tsivadze, A. Bessmertnykh-Lemeune and R. Guilard, *J. Porphyrins Phthalocyanines,* 2013, **17,** 1035–1045 (b) Z. Ou, J. Shen, J. Shao, M. Galezowski, D. T. Gryko and K. M. Kadish, *Inorg. Chem*., 2007, **46,** 2775-2786. (c) J. Shen, Z. Ou, J. Shao, M. Galezowski, D. T. Gryko and K. M. Kadish, *J. Porphyrins Phthalocyanines,* 2007, **11**, 269-276. (d) Z. Ou, H. Suna, H. Zhua, Z. Daa and K. M. Kadish, *J. Porphyrins Phthalocyanines,* 2008, **12,** 1-10.

33. J. Shen, J. Shao, Z. Ou, B. Koszarna, D. T. Gryko and K. M. Kadish, *Inorg. Chem.,* 2006, **45,** 2251-2265.
34. J. P. Gisselbrecht, M. Gross, E. Vogel and S. Will, *J. Electroanal. Chem.,* 2001, **205**, 170-172.
35. A. Mahammed, J. J. Weaver, H. B. Gray, M. Abdelas and Z. Gross, *Tetrahedron. Lett.,* 2003, **44,** 2077-2079.
36. R. Grigg, R. J. Hamilton, M. L. Jozefowicz, C. H. Rochester, R.J. Terrell and H. Wickwar, *J. Chem. Soc., Perkin Trans. 2,* 1973, **2,** 407-413.
37. M. J. Broadhurst, R. Grigg and G. J. Shelton, *Chem. Soc., Perkin Trans. 1,* 1972, 143-151.
38. P. E. Ellis, J. E. Linard, T. Szymanski, R. D. Jones, J. R. Budge and F. Basolo, *J. Am. Chem. Soc.,* 1980, **102,** 1889-1896.
39. C. Y. Li, X. B. Zhang, Z. X. Han, B. A. Kermark, L. Sun, G. L. Shena and R. Q.Yua, *Analyst,* 2006, **131**, 388–393.
40. Y. Zhang, M. X. Li, M.Y. Lu, R.H. Yang, F. Liu and K. A. Li, *J. Phys. Chem. A,* 2005, **109,** 7442-7448.
41. F. Zhi, X. Lu, J. Yang, X. Wang, H. Shang, S. Zhang and Z. Xue, *J. Phys. Chem. C* , 2009, **113,** 13166–13172. (b) P. Kubat, K. Lang and P. Anzenbacher, *Biochim. Biophys. Acta,* 2004, **1670,** 40-48.
42. J. M. M. Rodrigues, A. S. F. Farinha, F. P. V. Muteto, S. M. Woranovicz-Barreira, F. A. A. Paz, M. G. P. M. S. Neves, J. A. S. Cavaleiro, A. C. Tome, M. T. S. R. Gomes, J. L. Sessler and J. P.C. Tome, *Chem. Commun*., 2014, **50,** 1359-1361.
43. V. M. Patel, J. A. Patel, S. S. Havele and S. R. Dhaneshwar, *Int. J. Chem. Tech. Res*., 2010, **2,** 756-761
44. (a) J. P. Collman, J. I. Brauman, K. M. Doxsee, T. R. Halbert, S. E. Hayes and K. S. Suslick, *J. Am. Chem. Soc*., 1978, **100**, 2761-2766 (b) K. S. Suslick, M. M. Fox and T. J. Reinert, *J. Am. Chem. Soc*., 1984, **106**, 4522-4525.
45. (a) A. V. Hill, *J. Physiol. London*, 1910, **40**, IV-VII (b) C. A. Hunter, M. N. Meah and J. K. M. Sanders, *J. Am. Chem. Soc*., 1990, **112**, 5773-5780.
46. S. K. Hau, Y. J. Cheng, H. L. Yip, Y. Zhang, H. Ma and A. K. Y. Jen, *Appl. Mater. Interfaces,* 2010, **2,** 1892-1902.
47. A. Alemayehu, J. Conradie and A. Ghosh, *Eur. J. Inorg. Chem*., 2011, 1857-1864 (b) K. E. Thomas, A. B. Alemayehu, J. Conradie, C. Beavers, A. Ghosh, *Inorg. Chem*., 2011, **50,** 12844-12851.
48. A. K. Mahapatra, K. Maiti, P. Sahoo and P. K. Nandi, *J. Lumin.,* 2013, **143**, 349-354.

Graphical Abstract

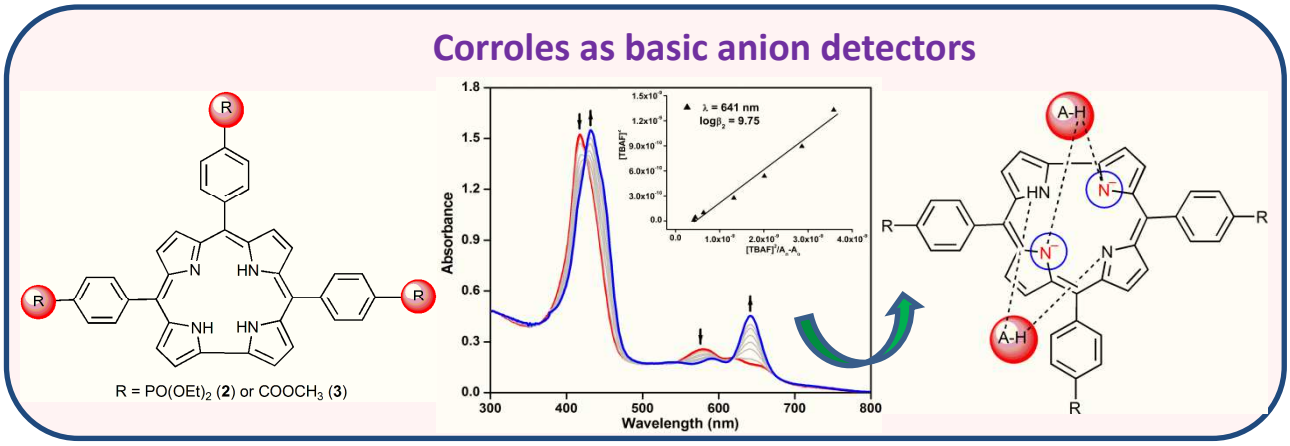

5,10,15-tris(4'-diethoxyphosphoryl/carbomethoxy-phenyl)corrole and their Cu(III) and Ag(III) complexes were synthesized. These metallocorroles have shown ~ 250 mV anodic shift in the first oxidation and ~ 100-150 mV in the metal centered reduction as compared to simple triphenylcorrole metal complexes. **2** and **3** have shown higher equilibrium constants with F^- ion (4.7×10^3 fold higher for **2** and 9.7×10^3 fold higher for **3**) as compared to **1** and being able to detect 0.06 µM of F^- ion with the limit of quantification (LOQ) 0.17 µM. Our results suggest that the electron deficient free base corroles can be utilized as basic anion detectors.

Table of Content (TOC)

Chart 1 Molecular structures of synthesized corroles.

Scheme 1 Synthesis of triphosphorylphenylcorrole (**2**) and its metal complexes (**2a** and **2b**).

Scheme 2 Schematic representation of protonation, deprotonation and anion binding with **1- 3**.

Fig. 1 (a) UV-Visible spectra of **2** and **2a-b** in CH_2Cl_2, (b) Fluorescence spectra of **2** and **3** in CH_2Cl_2.

Fig. 2 UV-Visible spectral titration of **2** (2.13×10^{-5} M) with µM concentration of TFA in acetonitrile. Inset shows a plot between [TFA] and $[TFA]/(A_n-A_0)$.

Fig. 3 UV-Visible spectral changes in **2** (2.59×10^{-5}M) during addition of TBAOH in acetonitrile (inset shows a plot between $[TBAOH]^2$ and $[TBAOH]^2/(A_0-A_n)$).

Fig. 4 Absorption spectral changes of **2** with μM quantities of base and anion.

Fig. 5 UV-Visible titration of **2** (2.13×10^{-5} M) with TBAF (inset show a plot between $[TBAF]^2$ and $[TBAF]^2/(A_0-A_n)$).

Fig. 6 Cyclic Voltammograms of **1b-3b** in CH_2Cl_2 containing 0.1M TBAP (with a scan rate of 100 mV/s. GC Working electrode, Ag/AgCl Reference electrode and Pt wire counter electrode were used).

Fig. 7 The Plot of Hammet parameter (3σ) *versus* the first ring oxidation and the metal centered reduction of Cu(III) and Ag(III) complexes of **1** - **3**.

Table 1.Optical absorption spectral data[a] of compound **1-3** and their metal complexes in CH_2Cl_2.

Table 2 Protonation, deprotonation constant for **1** - **3** in CH_3CN at 298K.

Table 3 Equilibrium constants[a] of **1-3** while addition of μM quantities of anions in CH_3CN.

Table 4 Electrochemical redox data for compound 1-3 and their metal complexes in CH_2Cl_2.